

Geometric Design Method of Lightweight Line Gear Mechanism

Chao He¹ – Yangzhi Chen^{1,2} – Xiaoxiao Ping¹ ✉ – Zhen Chen¹ – Maoxi Zheng^{2,3} – Qinsong Zhang²

¹ Guangdong Ocean University, School of Mechanical and Energy Engineering, China

² South China University of Technology, School of Mechanical and Automotive Engineering, China

³ University of Electronic Science and Technology of China Zhongshan Institute, School of Mechanical and Electrical Engineering, China

✉ xiaoping.xiao@foxmail.com

Abstract Based on the space curve meshing theory, a lightweight line gear mechanism (LLGM) was proposed in this paper. The LLGM can achieve the objective of lightweight design by reducing the radial dimension of the gear, which has an improvement in terms of size reduction. The outstanding advantage of the LLGM is its ability to achieve a high transmission ratio. Three aspects were proposed to design the LLGM: first, the primary design method was obtained; second, an approach to simply and effectively establish the analytical model of the LLGM was presented, which showed that the lightweight characteristic of the LLGM is mainly reflected in the radial dimension; third, the discriminant condition of the LLGM was built. The simplicity and effectiveness of the LLGM were demonstrated by a design example, while gear contact simulation and kinematics experiments were carried out to verify the theoretical basis. The lightweight design method proposed in this paper belonged to structural lightweight design, which can effectively solve the lightweight design issue in gear transmissions characterized by light loads and high transmission ratios.

Keywords lightweight design, space curve meshing, gear design, kinematics experiments, high transmission ratio

Highlights

- A novel lightweight line gear mechanism (LLGM) was proposed.
- The outstanding advantage of the LLGM is the high transmission ratio.
- The LLGM contributes to material amount savings.
- Kinematics experiments have been carried out on a homemade test rig.

1 INTRODUCTION

Gear transmission is widely recognized for its high meshing efficiency and reliability [1-4]. With the explosive growth of electromechanical products, the application of gears has become increasingly widespread [5]. Green transmission has emerged as a mainstream trend in the development of gears for the future. Achieving energy conservation and emission reduction has become a critical issue in the gear industry [6]. Among various solutions, structural lightweight design of gears has drawn the attention of many researchers and engineers [7-9]. Additionally, the miniaturization of electromechanical products has imposed higher requirements for lightweighting [10,11]. At present, lightweight gears have been important components in mini-electromechanical products, such as unmanned aerial vehicles and mini-robots [12,13].

Designing lightweight gears has been a key research issue for decades. In order to achieve the goal of lightweight, many design methods have been proposed. Some gears adopt a small module [14], others undergo topological optimization [15], and some are designed as specific gear devices [16,17]. Among the lightweight approaches, the simplest lightweight design method is to reduce the gear modulus and the number of teeth [18]. However, the load capacity of the gear decreases as the gear modulus decreases [19]. Besides, the teeth number of gears is normally not less than 17 to avoid undercut [20]. Therefore, the simplest lightweight gear design method is not universally effective. On the other hand, there are typically more than three gears when the transmission ratio of a gear device is more than 6 — a factor that obviously increases the difficulty of lightweight design due to the number of gears [21,22]. The lightweight gear pairs are also restricted by the radial dimension limitation of the two gears,

that is, the diameter of the driven gear is approximately equal to the product of the diameter of the driving gear and the transmission ratio. Once the diameter of one gear and the value of the transmission ratio are determined, the radial dimension of the other gear cannot be reduced. In summary, the previous lightweight designs leave room for improvement in terms of size reduction, especially under high transmission ratios.

To address the challenge of lightweight, this paper presents a lightweight design method based on a new theory. The method proposed in this paper belongs to structural design, and it can effectively address the challenge of lightweight design in mechanical transmissions with low-load and high-transmission-ratio characteristics. The research foundation of this paper primarily relies on the space curve meshing theory [23,24], called line gear (LG) [25]. Different from involute gears, LG can realize stable meshing transmission through two contact curves. Also, LG has the characteristics of a small number of teeth and no undercutting, making it suitable for lightweight design.

In this paper, a novel LG, named lightweight line gear mechanism (LLGM) is proposed. The LLGM can break through the radial dimension limitation of the two gears and achieve the objective of lightweight design by directly reducing the radial dimension of the gear, thereby achieving better size reduction performance than previous lightweight gears and LG. The design of the LLGM was proposed from three aspects: first, the primary design method was obtained through research; second, a simple approach for establishing the LLGM was presented; third, the discriminant condition of the LLGM was built. After that, a design example of the LLGM was put forward and a comparison was carried out between the LLGM and an ordinary LG pair. Gear contact simulation was carried out to

verify the contact characteristics. Finally, kinematics experiments were carried out to verify the proposed design theory. The LLGM is suitable for mini-electromechanical products, offering a new solution in mechanical transmissions characterized by high transmission ratios, lightweight design and compact size.

2 METHODS AND MATERIALS

2.1 Primary Design Parameters of the LLGM

The LLGM is build in accordance to the space curve meshing theory. Therefore, the LLGM mainly involves the design of two conjugate curves that present cylindrical helices [25], as shown in Fig. 1.

Two cylindrical helices denoted as A and B respectively, are rotated around their respective axes. Two fixed coordinate systems determine the relative position of curves A and B, and are named $O_1-x_1y_1z_1$ and $O_2-x_2y_2z_2$, respectively. The distance between them is expressed as a . The parameter equations of curves A and B were represented in the coordinate system $O_a-x_ay_az_a$ and $O_b-x_by_bz_b$, respectively. The $O_1-x_1y_1z_1$ and $O_2-x_2y_2z_2$ coincided with the $O_a-x_ay_az_a$ and $O_b-x_by_bz_b$ at the initial position. The curve A rotated through an angle φ_a at a uniform angular velocity ω_a and the curve B rotated through an angle φ_b at a uniform angular velocity ω_b while the two curves conducted conjugate motion.

Curves A and B can be expressed as Eqs. (1) and (2) in the coordinate system $O_a-x_ay_az_a$ and $O_b-x_by_bz_b$, respectively.

$$\mathbf{R}_a^a = \begin{cases} x_M^{(a)} = -m_a \cos t \\ y_M^{(a)} = m_a \sin t \\ z_M^{(a)} = n_a t \end{cases}, \quad (1)$$

$$\mathbf{R}_b^b = \begin{cases} x_M^{(b)} = m_b \cos t \\ y_M^{(b)} = m_b \sin t \\ z_M^{(b)} = n_b t \end{cases}, \quad (2)$$

wherein t is the independent variable, m_a and m_b represent the helix radius, n_a and n_b represent the pitch parameter.

The transformation matrix between the above coordinate systems can be expressed as:

$$\mathbf{M}_{21} = \begin{bmatrix} 1 & 0 & 0 & a \\ 0 & 1 & 0 & 0 \\ 0 & 0 & 1 & 0 \\ 0 & 0 & 0 & 1 \end{bmatrix}, \quad (3)$$

$$\mathbf{M}_{1a} = \begin{bmatrix} \cos \varphi_a & -\sin \varphi_a & 0 & 0 \\ \sin \varphi_a & \cos \varphi_a & 0 & 0 \\ 0 & 0 & 1 & 0 \\ 0 & 0 & 0 & 1 \end{bmatrix}, \quad (4)$$

$$\mathbf{M}_{2b} = \begin{bmatrix} \cos \varphi_b & -\sin \varphi_b & 0 & 0 \\ \sin \varphi_b & \cos \varphi_b & 0 & 0 \\ 0 & 0 & 1 & 0 \\ 0 & 0 & 0 & 1 \end{bmatrix}, \quad (5)$$

where \mathbf{M}_{21} , \mathbf{M}_{1a} and \mathbf{M}_{2b} represent the transformation relationship between the coordinate systems $O_1-x_1y_1z_1$ and $O_2-x_2y_2z_2$, $O_1-x_1y_1z_1$ and $O_a-x_ay_az_a$, $O_2-x_2y_2z_2$ and $O_b-x_by_bz_b$, respectively.

The equation of curve A can also be expressed in the coordinate system $O_1-x_1y_1z_1$ by Eq. (6), which defines rotation of curve A around the z_1 axis.

$$\mathbf{R}_1^1 = \mathbf{M}_{1a} \cdot \mathbf{R}_a^a. \quad (6)$$

The equation of the curve B can be similarly expressed in the coordinate system $O_2-x_2y_2z_2$ by Eq. (7), defining rotation of curve B around the z_2 axis.

$$\mathbf{R}_2^2 = \mathbf{M}_{2b} \cdot \mathbf{R}_b^b. \quad (7)$$

According to the conjugate condition, the curve A is tangent to the curve B while they are rotating, which can be expressed as:

$$\mathbf{R}_2^2 = \mathbf{M}_{21} \mathbf{R}_1^1. \quad (8)$$

The two sides of Eq. (8) represented the equations of the curve A and B in the coordinate system $O_2-x_2y_2z_2$. The solution to Eq. (8) is the position of the contact points of the two curves.

Further, Eq. (9) is obtained by substituting the known parameters into Eq. (8).

$$\begin{bmatrix} \cos \varphi_b & -\sin \varphi_b & 0 & 0 \\ \sin \varphi_b & \cos \varphi_b & 0 & 0 \\ 0 & 0 & 1 & 0 \\ 0 & 0 & 0 & 1 \end{bmatrix} \begin{bmatrix} m_b \cos t \\ m_b \sin t \\ n_b t \\ 1 \end{bmatrix} = \begin{bmatrix} 1 & 0 & 0 & a \\ 0 & 1 & 0 & 0 \\ 0 & 0 & 1 & 0 \\ 0 & 0 & 0 & 1 \end{bmatrix} \begin{bmatrix} \cos \varphi_a & -\sin \varphi_a & 0 & 0 \\ \sin \varphi_a & \cos \varphi_a & 0 & 0 \\ 0 & 0 & 1 & 0 \\ 0 & 0 & 0 & 1 \end{bmatrix} \begin{bmatrix} -m_a \cos t \\ m_a \sin t \\ n_a t \\ 1 \end{bmatrix}. \quad (9)$$

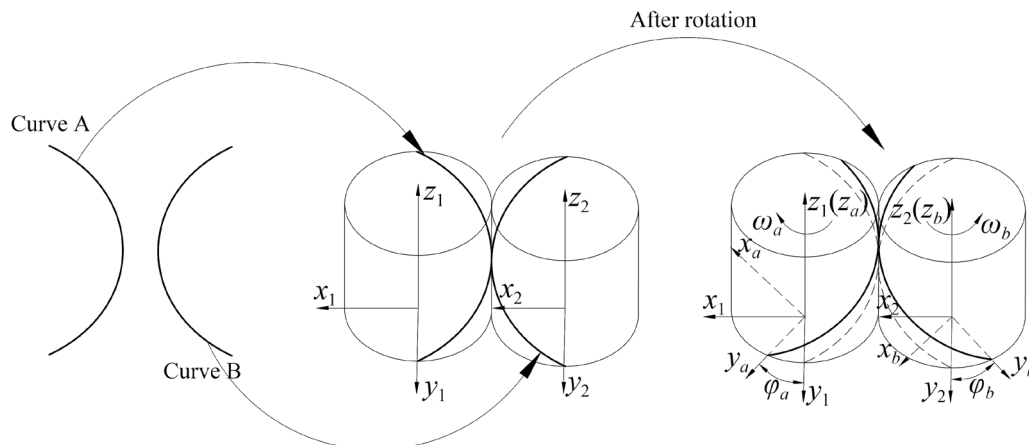


Fig. 1. Primary theory of the LLGM

At the initial position, φ_a and φ_b are both equal to 0. At other positions, the relationship between φ_a and φ_b is expressed as Eq. (10) by the gear transmission principle.

$$\varphi_a = i\varphi_b, \tag{10}$$

where i is the transmission ratio. By substituting the parameter i into Eq. (9), Eq. (11) can be obtained according to the space curve meshing theory.

$$i = \frac{n_b}{n_a}. \tag{11}$$

Equation (11) reveals the main factor influencing the transmission ratio of the LLGM, is the pitch ratio of the two curves.

2.2 Lightweight Design Method of the LLGM

Since the transmission ratio of the LLGM is directly related to the pitch ratio according to Eq. (11), the lightweight design of the LLGM can be mainly reflected in the radial dimension. A simple approach to establish the LLGM model was proposed for analysis, as shown in Fig. 2.

In Figure 2, the LG tooth was generated by sweeping, where the cylindrical helix was used as the path and the tooth profile was as used as the profile. There were two gear pairs, one was the ordinary LG and the other was the LLGM. As Figure 2 shows, both of the two gear pairs have the same driving gear, but the driven gear of the LLGM is smaller than that of the ordinary LG, while they have the same transmission ratio. In other words, the LLGM can achieve lightweight design by reducing the radial dimension.

2.3 Lightweight Condition of the LLGM

2.3.1 The Discriminant Condition of the LLGM

It can be seen from Fig. 2 that the LLGM and the ordinary LG have a similar structure. Therefore, it is necessary to introduce the discriminant condition of the LLGM. The main difference between the LLGM and the ordinary LG is the radial dimension. The change of the radial size brings a different sliding rate simultaneously. Therefore, the lightweight condition of the LLGM can be illustrated in terms of the sliding rate. According to the design theory of LG [26], the sliding rate can be calculated by Eq. (12).

$$S_r = 1 - \frac{\sqrt{n_b^2 + m_b^2}}{i\sqrt{n_a^2 + m_a^2}}, \tag{12}$$

where S_r represents the sliding rate. For the ordinary LG, the parameter m_b is approximately equal to im_a [26]. The relationship between the parameters n_a and n_b can be expressed as Eq. (11). Therefore, the sliding rate of the ordinary LG can be derived from Eq. (12).

$$S_{ro} \approx 0. \tag{13}$$

For the LLGM, the parameter m_b is smaller than im_a and the parameter n_b is equal to in_a . Therefore, $\sqrt{n_b^2 + m_b^2}$ is smaller than $i\sqrt{n_a^2 + m_a^2}$, and the sliding rate of the LLGM can be expressed as the inequality:

$$S_{rl} > 0, \tag{14}$$

where S_{rl} is the sliding rate of the LLGM. As shown in Eq. (13) and inequality in Eq. (14), the sliding rates of the LLGM and the ordinary LG are different. In short, the discriminant condition of the LLGM can be derived as follows.

1. $m_b < im_a$;
2. $S_r > 0$.

2.3.2 Degree of Lightweight of the LLGM

The degree of lightweight of the LLGM can be described by comparing the radial sizes of the LLGM and the ordinary LG. The degree of lightweight of the LLGM can be expressed as:

$$L_i = \left(100 \times \frac{im_a - m_b}{m_a + im_a} \right) \%, \tag{15}$$

The larger L_i , the greater the degree of lightweight. According to Eq. (12), the sliding rate increases with the degree of lightweight. Generally, the degree of lightweight of the LLGM is limited by sliding speed, which can be calculated by:

$$S_v = \frac{\pi n_r}{30} \left(\sqrt{n_a^2 + m_a^2} - \frac{\sqrt{n_b^2 + m_b^2}}{i} \right), \tag{16}$$

where S_v is the sliding speed of the LLGM, and n_r is the rotating speed of the driving wheel. The sliding speed can be selected according to the lubrication conditions [27]. Also, Eqs. (15) and (16)

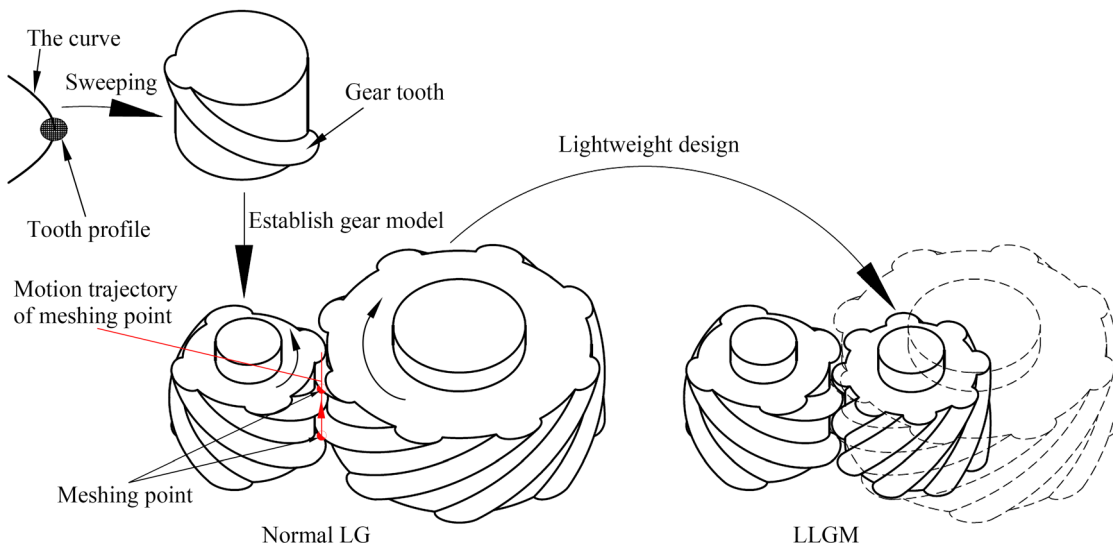


Fig. 2. Lightweight schematic of the LLGM

demonstrate that the LLGM maintains a sliding ratio greater than 0, with the sliding rate increasing as the degree of lightweight increases. In contrast, the sliding rate of LG gears remains constant and theoretically approaches zero, while the sliding rate of involute gears continuously varies throughout the meshing process and reverses direction at the pitch point. In short, the basic design method of the LLGM can be derived as follows:

1. Provide the conjugate curves according to the lightweight requirements;
2. Design the two gears;
3. Check the sliding speed.

2.4 Experimental

2.4.1 Design Example of the LLGM

An example of the LLGM was proposed to show the basic design method of the LLGM directly. For comparison, an ordinary LG pair was also proposed. The transmission ratios of the two gear pairs were both set to 8. The equations of the driving contact curves were set the same:

$$\mathbf{R}_a^a = \begin{cases} x_M^{(a)} = -10 \cos t \\ y_M^{(a)} = 10 \sin t \\ z_M^{(a)} = -12.7t \end{cases}, \quad (17)$$

where \mathbf{R}_a^a represents the equation of the driving contact curves. In this example, to achieve over 50 % lightweighting, the equations of the contact curves for the driven gears are as follows:

$$\mathbf{R}_b^b = \begin{cases} x_M^{(b)} = 27.5 \cos t \\ y_M^{(b)} = 27.5 \sin t \\ z_M^{(b)} = -101.6t \end{cases}, \quad (18)$$

$$\mathbf{R}_c^c = \begin{cases} x_M^{(c)} = -80 \cos t \\ y_M^{(c)} = 80 \sin t \\ z_M^{(c)} = -101.6t \end{cases}, \quad (19)$$

where \mathbf{R}_b^b represents the equation of the contact curves on the driven gear of the LLGM and \mathbf{R}_c^c represents the equation of the contact curves on the ordinary driven LG.

Next, the tooth profile was set as a rounded equilateral triangle with a height of 2.5 mm and a fillet diameter of 1 mm; the tooth width was set to 40 mm; the tooth numbers of the ordinary LG pair were set to 4 (driving gear) and 32 (driven gear), while those of the LLGM were set to 2 (driving gear) and 16 (driven gear), respectively. The geometry of the LG resembles that of a worm, and among its parameters, the pitch parameter is the most critical. Specifically, the pitch values of the driving LG and the driven LG were set to 40 mm and 320 mm, respectively.

The 3D models of the two gear pairs can be obtained according to the above settings. The main difference between the two gear pairs lies in the two driven gears, as shown in Fig. 3.

The comparison between the ordinary LG pair and the LLGM was conducted, some comparative parameters were tabulated as shown in Table 1.

Table 1. Comparisons between different gear pairs

Comparative items	The ordinary LG pair	The LLGM
Transmission ratio	8	8
Number of gears	2	2
Material amount [cm ³]	681	120

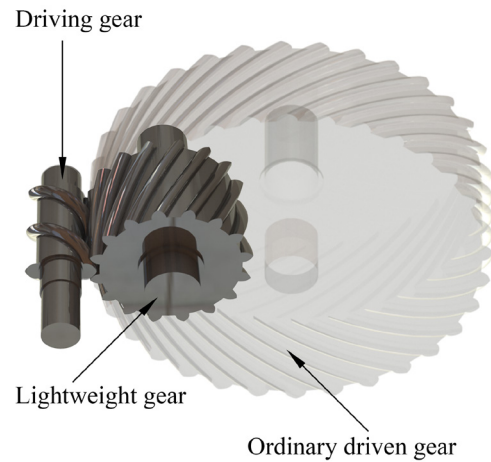


Fig. 3. Model of the design example

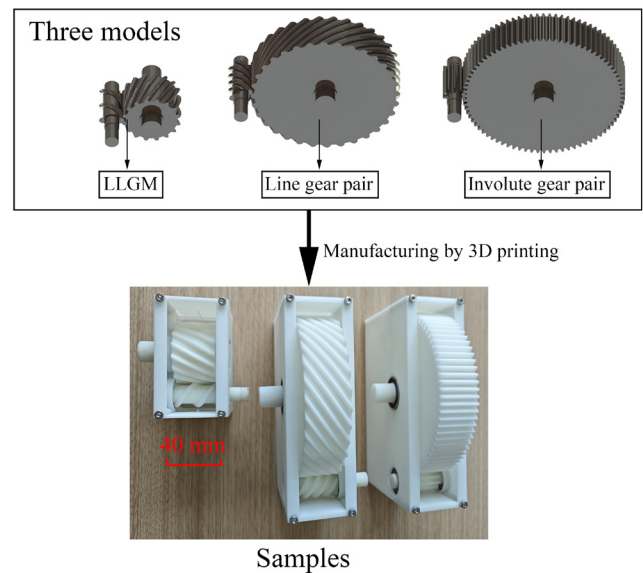


Fig. 4. The three reducers

According to Eq. (15), the degree of lightweight of the LLGM design example was equal to 58.33 %. As shown in Table 1, the LLGM achieves significant lightweighting, saving 82.37 % material usage compared with the ordinary LG.

2.4.2 Testing of the LLGM Reducer

For the convenience of analysis, an involute gear pair was also proposed. The modulus of the involute gear was set to 2 mm since the LG tooth size was equivalent to 2 mm modulus. For the involute gear, the tooth width was set to 40 mm; the tooth numbers were set to 10 (driving gear) and 80 (driven gear). The three reducers were designed on the basis of the above settings and then manufactured by 3D printing technology, as shown in Fig. 4.

The three reducers (LLGM reducer, LG reducer and involute gear reducer) were successively installed on a homemade test rig for kinematics experiments, as shown in Fig. 5.

Subsequently, kinematics experiments were carried out to test the performance of the three reducers on the homemade test rig, following the experimental methodology detailed in [28]. During the testing, the servo motor provided rotational speed to the reducer while the magnetic brake applied the load. The speed data were collected by the two encoders fixed on the input and output shafts, respectively.

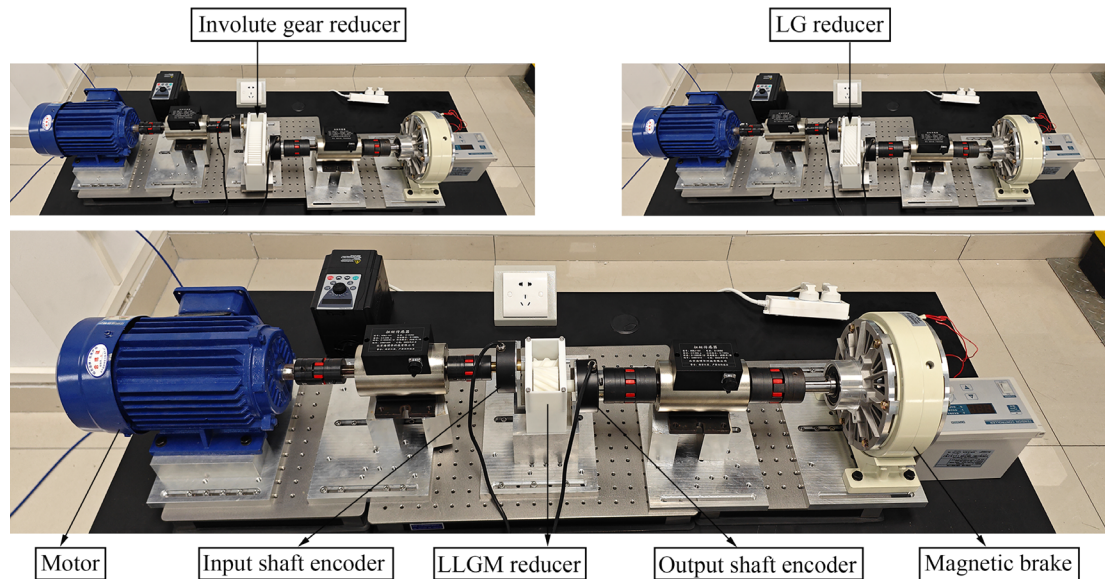


Fig. 5. Testing for the three reducers

The input speed was set to 750 r/min, the sampling frequency of the encoder was set to 10 Hz, and the load was set to 1 N·m.

3 RESULTS AND DISCUSSION

The experimental results were obtained after conducting the tests with the given experimental parameters. The transmission ratio data was obtained from the collected speed data. The transmission ratio diagram was drawn after using the six-point median filtering in data processing [25], as shown in Fig. 6. Then, according to the collected transmission ratio data, the error analysis was carried out, as shown in Table 2. Furthermore, simulation analysis was carried out for the three gear drives in ANSYS software, and the tooth surface contact stress results were shown in Fig. 7.

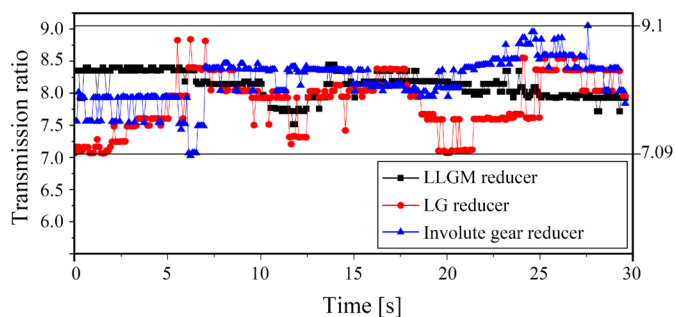


Fig. 6. Transmission ratio diagram of the three reducers

Table 2. Some transmission ratio errors of the three reducers

Comparative items	LLGM reducer	LG reducer	Involute gear reducer
Average transmission ratio	8.006	7.988	8.031
Standard deviation	0.192	0.423	0.340
Range error	0.903	1.811	1.970

According to the simulation results in Fig. 7, both the LLGM and LG exhibit point contact, while involute gears feature line contact. The contact points of the LLGM are distributed along the tooth direction position parallel to the axis, and the trajectory of the meshing points is consistent with that shown in Fig. 2.

The main experimental results (Fig. 6 and Table 2) indicate that the three reducers exhibit similar transmission ratio errors, demonstrating comparable kinematic performance. The results also show that the LLGM can realize stable transmission with a high transmission ratio, which explains the correctness of the geometric design method of the LLGM directly. During the testing, the input speed was given based on the rated speed of the motor. According to the Eq. (16), the sliding speed of the LLGM reducer was calculated as $0.314n_p$, which can inform speed limitations or lubrication design. However, there were considerable transmission errors during the testing mainly due to manufacturing error. These errors could be mitigated through improved manufacturing precision. According to the simulation results, the contact stress of the LLGM is greater than that of the other two gears, which is unfavorable for its load bearing capacity. There are two key factors accounting for the relatively high contact stress. One is the presence of point contact, and the other is the lack of tooth profile optimization in the LLGM design. Despite using a simple tooth profile, we proved the geometric feasibility of its design. The simplicity and effectiveness of the LLGM were demonstrated by kinematics experiments and simulation analysis.

Furthermore, floor cleaning robot gearbox composed of four-stage involute gear pairs was used for comparison with the LLGM reducer, as shown in Fig. 8. The main comparisons between the LLGM reducer and the floor cleaning robot gearbox were shown in Table 3. As shown in Table 3, the LLGM reducer achieves a 48% volume reduction and a 50% reduction in the number of gears compared with the floor cleaning robot gearbox. Overall, the LLGM demonstrates significant advantages in lightweight design and high transmission ratio capability, which are especially suitable for small-scale electromechanical products.

Table 3. Comparisons between the LLGM reducer and the floor cleaning robot gearbox

Comparative items	The LLGM reducer	The floor cleaning robot gearbox
Modulus [mm]	0.5	0.5
Transmission ratio	64	62.24
Number of gears	4	8
Overall size [mm]	43 × 28 × 21	85 × 36 × 16

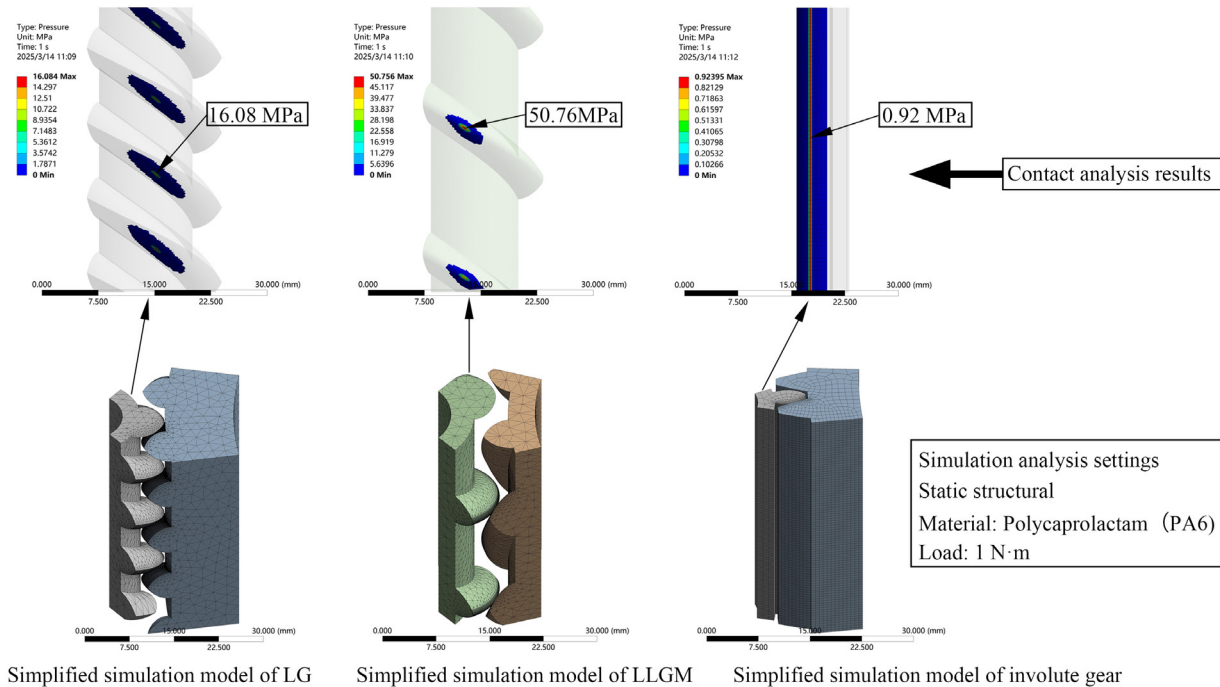


Fig. 7. Simulation analysis of tooth surface contact conditions



Fig. 8. The floor cleaning robot gearbox

4 CONCLUSIONS

In this paper, a lightweight line gear mechanism (LLGM) was proposed, and the main work is summarized as follows:

1. Based on the theory of space curve meshing, the geometric design method of the LLGM was studied, while the lightweight objective was achieved by directly reducing the radial dimensions of gears.
2. An approach to establish a simple and effective analytical model of the LLGM was presented. The outstanding advantage of the mechanism is its ability to obtain a high transmission ratio in a compact size.

3. An LLGM example was given, and experimental tests were conducted. The results proved that the LLGM reducer can achieve as stable transmission as other gear transmissions under light loads.

It has been verified that the geometric design method of the LLGM is correct and that the methodology can provide new solutions for the lightweight design mechanical transmissions. However, numerous challenges remain; such as torque measurement, lubrication optimization, strength characterization, dynamic response analysis, and precision manufacturing requirement. We aim to carry out more in-depth studies in the future to solve these problems.

Nomenclature

$O_1-x_1y_1z_1$	Reference coordinate system for driving gear
$O_2-x_2y_2z_2$	Reference coordinate system for driven gear
$O_a-x_a y_a z_a$	Body coordinate system of driving gear
$O_b-x_b y_b z_b$	Body coordinate system of driven gear
ω_a	Uniform angular velocity of driving gear, [rad /s]
ω_b	Uniform angular velocity of driven gear, [rad /s]
m_a	Helix radius of driving space curve, [mm]
m_b	Helix radius of driven space curve, [mm]
n_a	Parameters related to driving space curve pitch, [mm]
n_b	Parameters related to driven space curve pitch, [mm]
i	Transmission ratio
n_r	Rotating speed, [r/min]
t	Independent variable
φ_a	Rotation angle of driving gear, [rad]
φ_b	Rotation angle of driven gear, [rad]
\mathbf{M}_{21}	Transformation matrix between $O_2-x_2y_2z_2$ and $O_1-x_1y_1z_1$
\mathbf{M}_{1a}	Transformation matrix between $O_1-x_1y_1z_1$ and $O_a-x_a y_a z_a$
\mathbf{M}_{2a}	Transformation matrix between $O_2-x_2y_2z_2$ and $O_b-x_b y_b z_b$
\mathbf{R}_a^a	Equation of driving space curve in $O_a-x_a y_a z_a$
\mathbf{R}_b^b	Equation of driven space curve in $O_b-x_b y_b z_b$
\mathbf{R}_1^1	Equation of driving space curve in $O_1-x_1y_1z_1$
\mathbf{R}_2^2	Equation of driven space curve in $O_2-x_2y_2z_2$
S_{ro}	Sliding rate of the ordinary LG
S_f	Sliding rate
S_{fl}	Sliding rate of the LLGM
L_i	Degree of lightweight
S_v	Sliding speed, [m/s]
\mathbf{R}_c	Equation of driven space curve for ordinary LG

References

- [1] Wang, C. Study on dynamic performance and optimal design for differential gear train in wind turbine gearbox. *Renew Energ* 221, 119776 (2024) DOI:10.1016/j.renene.2023.119776.
- [2] Okorn, I., Nagode, M., Klemenc, J. Operating performance of external non-involute spur and helical gears: A review. *Stroj vestn-J Mech E* 67 (2021) DOI:5545/sv-jme.2020.7094.
- [3] Zhang, Y., Zhou, H., Duan, C., Wang, Z., Luo, H. Gear differential flank modification design method for low noise. *Stroj vestn-J Mech E* 70 569-581 (2024) DOI:10.5545/sv-jme.2024.1072.
- [4] Dong, C., Yang, X., Li, D., Zhao, G., Liu, Y. Service performance optimization and experimental study of a new WW type non-circular planetary gear train. *Stroj vestn-J Mech E* 70 128-140 *Stroj vestn-J Mech E* 70 128-140 (2024) DOI:10.5545/sv-jme.2023.673.
- [5] Litvin, F.L., Fuentes, A. *Gear Geometry and Applied Theory*. Cambridge University Press (2004) New York, DOI:10.1017/CB09780511547126.
- [6] Pingkuo, L., Huan, P. What drives the green and low-carbon energy transition in China?: An empirical analysis based on a novel framework. *Energy* 239 122450 (2022) DOI:10.1016/j.energy.2021.122450.
- [7] Cosco, F., Adduci, R., Muzzi, L., Rezayat, A., Mundo, D. Multiobjective design optimization of lightweight gears. *Machines* 10 779 (2022) DOI:10.3390/machines10090779.
- [8] Ide, T., Kitajima, H., Otomori, M., Leiva, J.P., Watson, B.C. Structural optimization methods of nonlinear static analysis with contact and its application to design lightweight gear box of automatic transmission of vehicles. *Struct Multidiscip O* 53 1383-1394 (2016) DOI:10.1007/s00158-015-1369-y.
- [9] Wang, D., Shen, H., Dong, H., Yu, S. A novel approach for conceptual structural design of gearbox. *Mechanisms, Transmissions and Applications: Proceedings of the 3rd MeTrApp Conference* (2015) 177-185, DOI:10.1007/978-3-319-17067-1_19.
- [10] Tezel, T., Schultheiss, U., Hornberger, H., Kovan, V. Operational wear behaviour of 3D-printed lightweight metal gears: EDS and oil analysis comparison. *Mater Test* 66 830-834 (2024) DOI:10.1515/mt-2023-0222.
- [11] Wu, J., Wei, P., Zhu, C., Zhang, P., Liu, H. Development and application of high strength gears. *Int J Adv Manuf Tech* 132 3123-3148 (2024) DOI:10.1007/s00170-024-13479-x.
- [12] Zhao, X., Zhou, Z., Zhu, X., Guo, A. Design of a hand-launched solar-powered unmanned aerial vehicle (UAV) system for plateau. *Appl Sci-Basel* 10 1300 (2020) DOI:10.3390/app10041300.
- [13] Zheng, C., Lee, K. WheelLeR: Wheel-leg reconfigurable mechanism with passive gears for mobile robot applications. *2019 International Conference on Robotics and Automation* (2019) 9292-9298 DOI:10.1109/ICRA.2019.8793686.
- [14] Concli, F. Tooth root bending strength of gears: dimensional effect for small gears having a module below 5 mm. *Appl Sci* 11 2416 (2021) DOI:10.3390/app11052416.
- [15] Ramadani, R., Pal, S., Kegl, M., Predan, J., Drstvenšek, I., Pehan, S., Belšak, A. Topology optimization and additive manufacturing in producing lightweight and low vibration gear body. *Int J Adv Manuf Tech* 113 3389-3399 (2021) DOI:10.1007/s00170-021-06841-w.
- [16] Chang, J., Chang, I. Design of high ratio gear reducer using vernier differential theory. *J Mech Design*, 143 023401 (2021) DOI:10.1115/1.4047347.
- [17] Mo, J., Gong, X., Luo, S., Fu, S., Chang, X., Liao, L. Geometric design and dynamic characteristics of a novel abnormal cycloidal gear reducer. *Adv Mech Eng* 15 16878132231158895 (2023) DOI:10.1177/16878132231158895.
- [18] Hsueh-Cheng, Y., Huang, Z.W. Using variable modulus to modify a rack cutter and generate a gear pair. *P I Mech Eng C-J Mec* 236 5342-5359 (2022) DOI:1177/09544062211061711.
- [19] Mo, S., Zhou, C., Zhang, W., Liu, Z., Hu, X., Bao, H., et al. Study on small modulus modified gear damage fault and electromechanical coupling vibration characteristics under multiple working conditions. *P I Mech Eng C-J Mec* 238 3746-3774 (2024) DOI:1177/09544062231207440.
- [20] Alipiev, O., Antonov, S., Grozeva, T. Generalized model of undercutting of involute spur gears generated by rack-cutters. *Mech Mach Theory* 64 39-52 (2013) DOI:1016/j.mechmachtheory.2013.01.012.
- [21] Xin, W., Zhang, Y., Fu, Y., Yang, W., Zheng, H. A multi-objective optimization design approach of large mining planetary gear reducer. *Sci Rep-UK* 13 18640 (2023) DOI:1038/s41598-023-45745-5.
- [22] Sun, G.B., Chiu, Y.J., Zuo, W.Y., Zhou, S., Gan, J.C., Li, Y. Transmission ratio optimization of two-speed gearbox in battery electric passenger vehicles. *Adv Mech Eng* 13 16878140211022869 (2021) DOI:1177/16878140211022869.
- [23] Chen, Z., Chen, Y.Z., Ding, J. A generalized space curve meshing equation for arbitrary intersecting gear. *P I Mech Eng C-J Mec* 227 1599-1607 (2013) DOI:1177/0954406212463310.
- [24] Chen, Y.Z., He, C., Lyu, Y.L. Basic theory and design method of variable shaft angle line gear mechanism. *Stroj vestn-J Mech E* 67 352-362 (2021) DOI:5545/sv-jme.2021.7216.
- [25] Chen, Y.Z., Huang, H., Lv, Y. A variable-ratio line gear mechanism. *Mech Mach Theory* 98 151-163 (2016) DOI:1016/j.mechmachtheory.2015.12.005.
- [26] Chen, Y., Li, Z., Xie, X., Lyu, Y. Design methodology for coplanar axes line gear with controllable sliding rate. *Stroj vestn-J Mech E* 64 (2018) DOI:5545/sv-jme.2017.5110.
- [27] Chen, Y., Chen, H., Lyu, Y., Zhu, A. Study on geometric contact model of elastohydrodynamic lubrication of arbitrary intersecting line gear. *Lubr Sci* 30 387-400 (2018) DOI:1002/ls.1429.
- [28] He, C., Chen, Y., Lin, W., Lyu, Y. Research on the centre distance separability of parallel shaft line gear pair. *P I Mech Eng C-J Mec* 236 3261-3274 (2022) DOI:10.1177/09544062211035809.

Acknowledgements This research was supported by program for Zhanjiang Science and Technology Plan Project (No.2024B01054 and 2024B01042); and scientific research start-up funds of Guangdong Ocean University (Grant No. YJR23010, YJR23002, YJR22016, and YJR24019); National Natural Science Foundation of China (Grant No. 52275073 and 52405056); and Open Fund of Guangdong Provincial Key Laboratory of Precision Gear Flexible Manufacturing Equipment Technology Enterprises, Zhongshan MLTOR Numerical Control Technology Co., LTD & South China University of Technology (No. 2021B1212050012-08).

Received: 2024-10-04, **revised:** 2025-03-15, **accepted:** 2025-04-10 as Original Scientific Paper

Data Availability The data supporting the findings of this study are included in the article.

Author Contribution Chao He: Methodology, Formal Analysis, Validation, Writing – original draft. Yangzhi Chen: Conceptualization, Supervision. Xiaoxiao Ping: Conceptualization, Methodology, Resources, Formal Analysis. Zhen Chen: Writing – review & editing, Supervision. Qinsong Zhang: Formal analysis, Investigation, Writing – review & editing.

Geometrijska metoda zasnove lahkega linijskega zobniškega mehanizma

Povzetek Na osnovi teorije ozobljenja prostorskih krivulj je v tem članku predstavljen lahek linijski zobniški mehanizem (LLZM). LLZM omogoča dosego lahke konstrukcije z neposrednim zmanjšanjem radialne mere zobnika, kar zagotavlja pomembno izboljšavo glede zmanjšanja velikosti.

Posebna prednost LLZM je možnost doseganja visokih prenosnih razmerij. Za zasnovo LLZM so bili predlagani trije vidiki: prvič, določena je bila osnovna metoda zasnove; drugič, predstavljena je bila enostavna in učinkovita metoda vzpostavitve analitičnega modela LLZM, ki je pokazala, da se lahka zasnova LLZM odraža predvsem v zmanjšanju radialnih mer; tretjič, postavljen je bil kriterij za presojo ustreznosti LLZM. Preprostost in učinkovitost LLZM sta bila prikazana s konkretnim primerom zasnove ter preverjena s simulacijo zobniškega stika in kinematičnimi poskusi, ki potrjujejo teoretične osnove. Metoda zasnove, predstavljena v tem članku, spada med strukturne metode lahke zasnove in učinkovito rešuje problem lahkih zobniških prenosov, ki prenašajo majhne obremenitve in zagotavljajo visoka prenosna razmerja.

Ključne besede lahka zasnova, ozobljenje prostorske krivulje, zasnova zobnikov, kinematični poskusi, visoko prenosno razmerje